An Oncogenomics-Based In Vivo RNAi Screen Identifies Tumor Suppressors in Liver Cancer

Lars Zender,[1,6,7] Wen Xue,[1,7] Johannes Zuber,[1] Camile P. Semighini,[1] Alexander Krasnitz,[1] Beicong Ma,[1] Peggy Zender,[1] Stefan Kubicka,[3] John M. Luk,[4] Peter Schirmacher,[5] W. Richard McCombie,[1] Michael Wigler,[1] James Hicks,[1] Gregory J. Hannon,[1,2] Scott Powers,[1] and Scott W. Lowe[1,2,*]

[1]Cold Spring Harbor Laboratory
[2]Howard Hughes Medical Institute
Cold Spring Harbor, New York 11724, USA
[3]Department of Gastroenterology and Hepatology, Medical School Hannover, 30625 Hannover, Germany
[4]Department of Surgery, University of Hong Kong, Hong Kong, China
[5]Institute of Pathology, University Hospital Heidelberg, 69120 Heidelberg, Germany
[6]Present address: Helmholtz Centre for Infection Research (HZI), 38124 Braunschweig, Germany and Department of Gastroenterology, Hepatology and Endocrinology, Medical School Hannover, 30625 Hannover, Germany
[7]These authors contributed equally to this work
*Correspondence: lowe@cshl.edu
DOI 10.1016/j.cell.2008.09.061

SUMMARY

Cancers are highly heterogeneous and contain many passenger and driver mutations. To functionally identify tumor suppressor genes relevant to human cancer, we compiled pools of short hairpin RNAs (shRNAs) targeting the mouse orthologs of genes recurrently deleted in a series of human hepatocellular carcinomas and tested their ability to promote tumorigenesis in a mosaic mouse model. In contrast to randomly selected shRNA pools, many deletion-specific pools accelerated hepatocarcinogenesis in mice. Through further analysis, we identified and validated 13 tumor suppressor genes, 12 of which had not been linked to cancer before. One gene, *XPO4*, encodes a nuclear export protein whose substrate, EIF5A2, is amplified in human tumors, is required for proliferation of XPO4-deficient tumor cells, and promotes hepatocellular carcinoma in mice. Our results establish the feasibility of in vivo RNAi screens and illustrate how combining cancer genomics, RNA interference, and mosaic mouse models can facilitate the functional annotation of the cancer genome.

INTRODUCTION

Diversity and complexity are hallmarks of cancer genomes. Even tumors arising from the same cell type or tissue harbor a range of genetic lesions that facilitate their uncontrolled expansion and eventual metastasis. As a consequence, the behavior of individual tumors—how they progress and ultimately respond to therapy—is heterogeneous and unpredictable. To date, many cancer genes have been identified, and through characterization of their action, new treatment strategies have been established. It follows that a further understanding of cancer genetics will improve cancer diagnosis, prognosis, and therapy.

Recent technological advances have greatly increased the resolution and depth at which cancer cell genomes can be examined, making it possible to envision the cataloging of every gene whose mutation or alteration occurs in human tumors (Velculescu, 2008). For example, regions of copy number alteration can be identified by high-resolution array-based comparative genomic hybridization (CGH); in many cases, regions of chromosomal amplification harbor oncogenes, whereas deleted regions harbor tumor suppressor genes (Chin and Gray, 2008). In addition, somatic point mutations potentially selected for during tumor evolution can be identified by high-throughput sequencing (Wood et al., 2007; Greenman et al., 2007). However, owing to the inherent genomic instability of cancer cells, gene linkage, and spontaneous mutagenesis, cancers also contain somatically acquired "passenger" mutations that may not confer a selective advantage to the developing tumor. Moreover, some genes are haploinsufficient tumor suppressors, such that loss of even one allele can promote tumorigenesis—even without a corresponding mutation in the remaining wild-type allele—making it difficult to pinpoint relevant tumor suppressors in large deletions. Therefore, candidate genes identified through genomic approaches require functional validation before they are useful for clinical applications.

Functional characterization of cancer genes is often tedious, and it is not always obvious which assays will reveal the putative oncogenic activity of relatively uncharacterized genes. Moreover, although cell culture systems are tractable, in vitro models do not recapitulate all features of the tumor microenvironment and so do not survey all relevant gene activities. Currently, a "gold-standard" approach for studying candidate oncogenes and tumor suppressors involves the production of transgenic and knockout mice that contain germline alterations in the

candidate oncogenic lesion (Van Dyke and Jacks, 2002). These strains have proven invaluable for validating cancer genes and create powerful models for subsequent studies. Nevertheless, their generation and analysis is time consuming and expensive.

To facilitate a more rapid and cost-effective analysis of cancer gene action in vivo, we developed a "mosaic" mouse model of hepatocellular carcinoma (Zender et al., 2006), a common but understudied cancer for which there are few treatment options (Lee and Thorgeirsson, 2006; Teufel et al., 2007). In our mouse model, hepatocellular carcinomas (HCCs) with different oncogenic lesions can be rapidly produced by genetic manipulation of cultured embryonic liver progenitor cells (hepatoblasts) followed by their retransplantation into the livers of recipient mice (Zender et al., 2006; Zender et al., 2005). We have previously used this model to characterize the gene products contained in the 11q22 amplicon observed in human tumors and showed that both *YAP1* and *cIAP1* cooperate to promote tumorigenesis in particular genetic contexts (Zender et al., 2006).

To further accelerate the study of cancer genes in vivo, our laboratory has adapted stable RNA interference (RNAi) technology to downregulate tumor suppressor genes in mice (Hemann et al., 2003). We utilize microRNA-based short hairpin RNAs (shRNAmir, hereafter referred to as shRNAs) that are potent triggers of the RNAi machinery and can efficiently suppress gene expression when expressed from a single genomic copy (Dickins et al., 2005; Silva et al., 2005). We previously used this technology in our mosaic mouse model of hepatocellular carcinoma to show that stable knockdown of the *p53* tumor suppressor by RNAi can mimic *p53* gene loss in vivo (Zender et al., 2005) and that regulated RNAi can reversibly modulate endogenous p53 expression to implicate the role of p53 loss in tumor maintenance (Xue et al., 2007). We also used similar approaches to rapidly validate *Deleted in Liver Cancer 1* (*DLC1*) as a potent tumor suppressor gene (Xue et al., 2008).

The goal of this study was to integrate cancer genomics, RNAi technology, and mouse models to rapidly discover and validate cancer genes. Our approach was based on the premise that genomic deletions occurring in human tumors should be enriched for tumor suppressor genes. We therefore produced a focused shRNA library targeting the mouse orthologs of genes deleted in human hepatocellular carcinoma and screened this for shRNAs that would promote tumorigenesis in our mosaic model of HCC. Our approach proved to be highly effective, resulting in the functional validation of 13 tumor suppressor genes. In addition to identifying new genes and pathways relevant to liver cancer and other tumor types, our study provides one blueprint for functionally annotating the cancer genome.

RESULTS

Oncogenomic Studies of Human Hepatocellular Carcinoma

Tumor suppressor gene inactivation is often due to homozygous or hemizygous chromosomal deletions. To identify genomic regions potentially containing tumor suppressor genes, we analyzed approximately 100 human hepatocellular carcinomas of different etiologies (Hepatitis B, Hepatitis C, or ethyltoxic liver cirrhosis) for DNA copy number alterations using representational oligonucleotide microarray analysis (ROMA), a high-resolution array-based CGH platform (Lucito et al., 2003). Raw data were converted into segmented profiles (Hicks et al., 2006), and segments that showed significant decrease from the ground state were identified (Figure 1A). We then computationally estimated genetic events so that a homozygous deletion within a heterozygous deletion would be scored as two deletion events rather than one (A.K., J.H., and M.W., unpublished data) and plotted the resulting deletion event frequency across the entire genome (Figure 1B). Among the many deletions detected, only a fraction were less then 5MB. We hypothesized that these focal deletions were most likely to be enriched for tumor suppressor genes.

To develop an initial gene list for further studies, we identified all of the genes embedded in recurrent focal deletions or in unique focal deletions whose gene content was also contained in broader deletions that were recurrent. On the basis of these criteria, we identified 58 deletions ranging in size from 98 kb to 2.6 Mb, containing 1 to 46 genes, respectively (see, for example, Figure 1C). Of the 362 annotated genes identified in total (Table S1 available online, see red circles in Figure 1B), we were able to bioinformatically identify 301 mouse orthologs. We next obtained all 631 of the mir30-based shRNAs from the Cold Spring Harbor Laboratory RNAi CODEX library. Thus, on average, each deleted gene was represented by approximately 2 murine shRNAs (see workflow in Figure S1A).

Constructing an In Vivo RNAi Screen

We recently developed a "mosaic" mouse model in which liver carcinomas can be rapidly produced by genetic manipulation of liver progenitor cells followed by their retransplantation into recipient mice (Zender et al., 2006). Since systemic delivery of RNAi currently does not enable efficient and stable knockdown of genes in tissues, we decided to introduce pools of shRNAs into premalignant progenitor cells and select for those that promote tumor formation after transplantation. We previously generated immortalized lines of embryonic hepatocytes lacking p53 and overexpressing Myc that were not tumorigenic in vivo (Zender et al., 2005); since over 40% of all human HCCs are overexpressing *MYC* and many harbor *p53* mutations or deletions (Teufel et al., 2007), we reasoned that these cells would provide a "sensitized" background where a single additional lesion might trigger tumorigenesis (Figure 2A).

We hypothesized that shRNAs targeting negative regulators of WNT signaling would provide positive controls to model or "reconstruct" our screen, as this pathway is deregulated in a significant percentage (30%–40%) of human hepatocellular carcinomas because of activating mutations in β-catenin or inactivating mutations or promoter hypermethylation of the *AXIN* and *APC* tumor suppressors (Teufel et al., 2007). We therefore introduced mir30-design shRNAs targeting *Axin* or *Apc* into $p53^{-/-}$; *Myc* hepatocytes and transplanted the resulting cell populations subcutaneously into nude mice or into the liver by intrasplenic injection (Zender et al., 2005, 2006). Of note, all of the shRNAs used in this study were cloned into pLMS, a vector optimized for in vivo use, which coexpresses green fluorescent protein (GFP) (Dickins et al., 2005). Furthermore, the *Myc* transgene coexpresses a luciferase reporter to facilitate monitoring of tumors with bioluminescence.
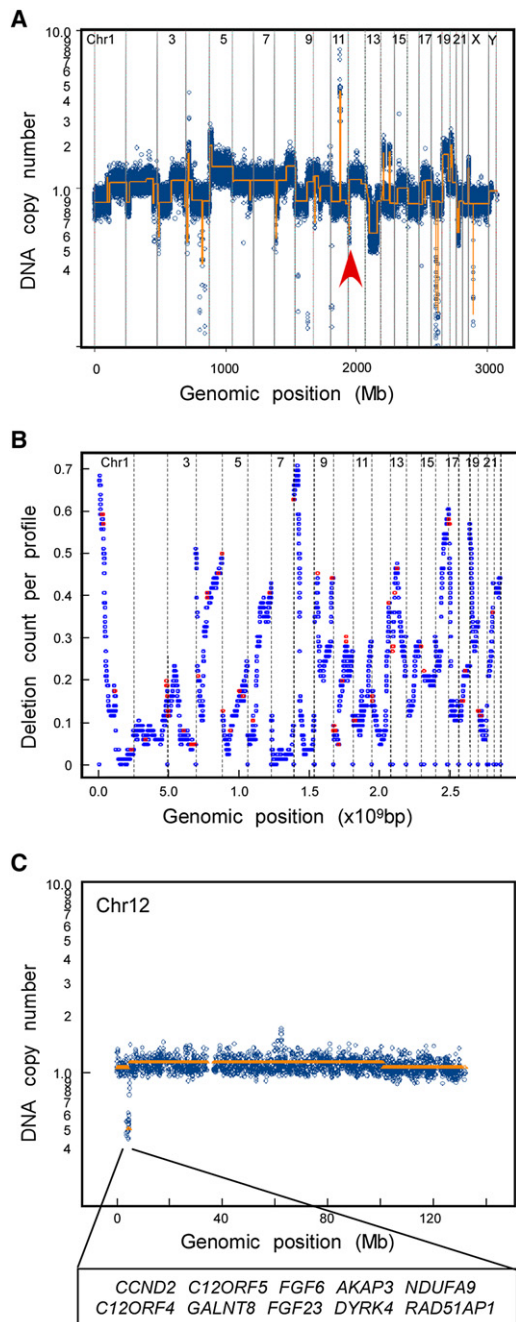
Figure 1. ROMA Deletion-Based RNA Interference Library

(A) A representative whole-genome ROMA array CGH plot of a human hepatocellular carcinoma (HCC). The arrow denotes the focal deletion highlighted in (C).

(B) Deletion counts in ROMA profiles of 98 human HCC. The points in the vicinity of 58 focal deletions (containing 362 genes) are highlighted by red circles. Dashed lines denote chromosome boundaries.

(C) A representative 524 Kb focal deletion on chromosome 12 contains ten genes.

Although a negative control shRNA (targeting human *RB1* but not mouse) did not trigger tumor growth, the positive control shRNAs targeting *Axin* or *Apc* gave rise to tumors within 1–2

months both subcutaneously and in situ (Figures 2A–2D). The resulting tumors were classified as aggressive solid, sometimes pseudoglandular, hepatocellular carcinomas (Figure 2D, top panel). They also displayed high levels of nuclear β-catenin by immunohistochemistry, indicating that the shRNAs were deregulating the predicted biochemical pathway (Figure 2D, bottom panel).

In order to determine the complexity of shRNA pools that could be screened, we tested one *Apc* shRNA for its ability to accelerate tumorigenesis when diluted 1:10 to 1:100. In addition, we tested a pool of 48 shRNAs targeting various murine genes that also contained two distinct *Apc* shRNAs. In both situations, the diluted shRNAs produced tumors rapidly, albeit with a delay relative to the pure *Apc* shRNA (Figure 2E). Moreover, sequencing of PCR-amplified shRNAs obtained from tumors triggered by the shRNA pool indicated that the two *Apc* shRNAs were enriched during tumor expansion, comprising the majority of shRNAs present in the resulting tumors (data not shown). Thus, pools of 48 shRNAs can be readily screened to identify those with tumor promoting activities similar to an *Apc* shRNA. Although 1:100 dilutions still enhanced tumor growth (data not shown), we concluded that screening of low complexity pools was feasible and would maximize our chances of identifying weaker shRNAs that might otherwise be outcompeted by stronger ones in more complex pools.

Many shRNA Pools Targeting Genes Deleted in Liver Cancer Promote Tumorigenesis In Vivo

To screen our shRNA library targeting deletion-associated genes, we pooled individual shRNAs randomly into pools of 48 and transferred them in bulk into pLMS (see also Figure S1B). Selected shRNA library pools were subjected to DNA sequencing to confirm that clone representation was maintained (data not shown). As controls, we also produced 10 pools of randomly selected shRNAs from the mouse CODEX RNAi library (i.e., not based on genomic location). Each pool, in parallel with a negative shRNA control, was introduced into $p53-/-;Myc$ hepatocytes at a low multiplicity of infection and the resulting cell populations were transplanted subcutaneously into both flanks of four immunocompromised mice. Animals were subsequently monitored for tumor development.

The results of these experiments were striking: while mice injected with cells transduced with randomly produced shRNA pools did not develop tumors over background (Figure 3A and Figure S2A), most mice transplanted with cells harboring the deletion-focused shRNA pools developed tumors, some within 3–4 weeks (Figure 3B and Figure S2B). Many tumors appeared to be multifocal and all were GFP positive, indicating that the tumor cells expressed at least one shRNA. These observations validate our enrichment strategy and suggest that deletion-focused shRNA libraries are enriched for tumor promoting shRNAs.

Identification of Candidate Tumor-Promoting shRNAs

To identify shRNAs present in tumors, we isolated genomic DNA from GFP-positive tumor nodules, PCR amplified the integrated shRNAs, and cloned them into a recipient vector that could also be used for subsequent validation (Figure 3C). As a cutoff criterion for further studies, we chose to isolate shRNAs from tumors
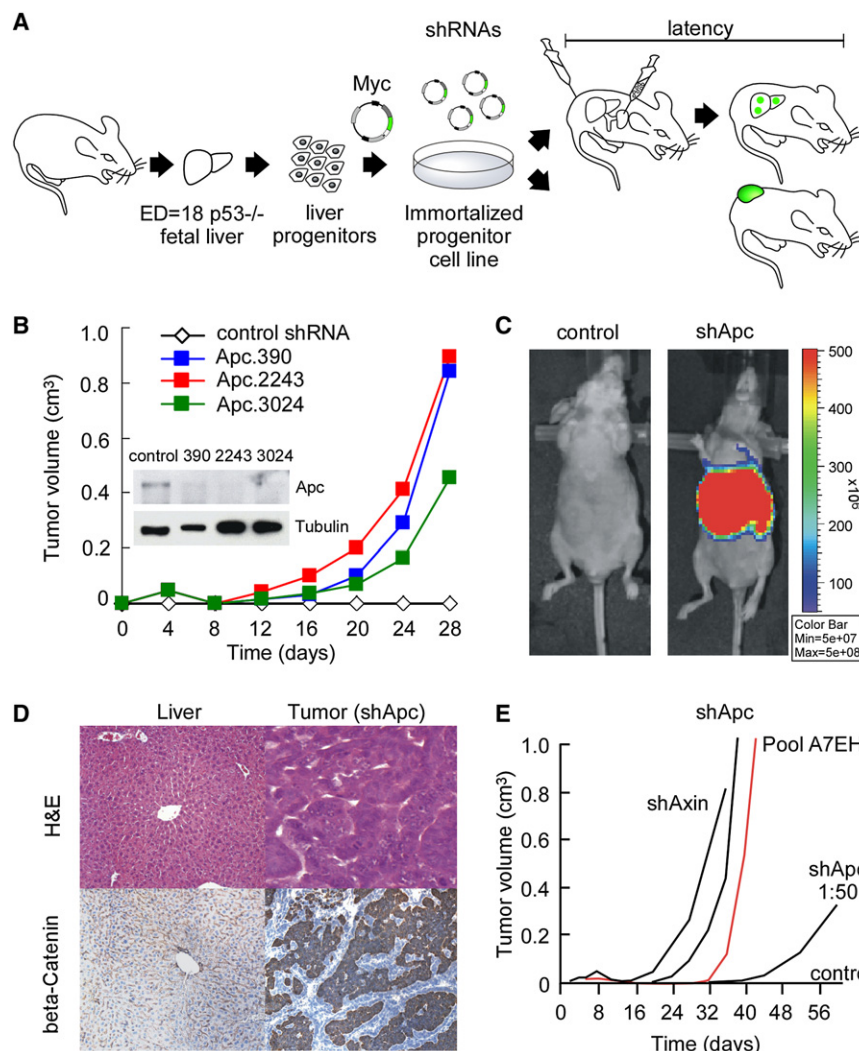
Figure 2. Setup of In Vivo RNA Interference Screening

(A) Schematic representation of the approach. E18 $p53^{-/-}$ liver progenitor cells are immortalized by transduction with a *Myc*-expressing retrovirus. Subsequently, the cells are infected with single shRNAs or shRNA library pools and injected into the liver or subcutaneously to allow tumor formation.

(B) Growth curve of tumors derived from $p53^{-/-}$; *Myc* cells infected with a control shRNA or three *Apc* shRNAs. Values are the average of six tumors. The inset shows knockdown of Apc protein assayed by western blot.

(C) Bioluminescence imaging of tumors derived from $p53^{-/-}$;*Myc* cells infected with a control shRNA or *Apc* shRNA and transplanted into the livers of immunocompromised recipient mice (n = 4). Animals were imaged 40 days after surgery.

(D) H&E and β-catenin staining of liver tumors in (C). Normal liver served as control.

(E) Tumor growth curve of $p53^{-/-}$;*Myc* cells infected with control shRNA (control), *Apc* shRNA (shAPC), a 1:50 diluted *Apc* shRNA (shAPC 1:50), *Axin* shRNA, and a shRNA library pool (pool A7EH, taken from the Cancer1000 library).

showed comparable levels of Pten knockdown and p-Akt (Figure 3G). Apparently, cells with optimal knockdown are selected from polyclonal populations during tumor expansion.

PTEN is a bona fide tumor suppressor gene that is mutated in many tumor types (Tokunaga et al., 2008) and whose deletion promotes hepatocarcinogenesis in mice (Horie et al., 2004). Accordingly, we identified several HCCs with either focal or broad chromosome 10 deletions encompassing *PTEN* (Figure 3E). To confirm that suppression of *Pten* is oncogenic in our model, we retested the recovered *Pten* shRNAs by introducing them into $p53^{-/-}$;*Myc* hepatocytes and testing their ability to form tumors after subcutaneous or intrasplenic injection. In both contexts, *Pten* knockdown rapidly triggered tumor growth (Figure 3F and Figure S3), thus validating our screening strategy and providing a blueprint for testing shRNAs targeting less characterized genes.

that were relatively large and derived from pools that efficiently accelerated tumorigenesis (average tumor volume $\geq$ 0.1cm³ and $\geq$ 50% take rate). None of the random shRNA pools fit these two criteria (Figures S2C and S2D). The resulting plasmid pools were then sequenced to determine the representation of particular shRNAs (96 sequence reads per tumor, more than three tumors per pool). In most cases, more than one shRNA was identified from each tumor nodule, suggesting that the tumors were multiclonal.

Interestingly, independent shRNAs targeting *Pten* were highly enriched in tumors produced from cells transduced with two different shRNA pools (Figure 3D). By comparing the relative representation of each *Pten* shRNA to that in the initial pool, we noted that Pten.932 (HP_524) was enriched from 3% to 41% during tumor expansion (Figure 3D, upper panel), whereas Pten.5331 (HP_465354) went from 1% to 67% of the total sequence reads (Figure 3D, lower panel). Immunoblotting revealed that both shRNAs suppressed Pten and increased Akt phosphorylation (Figure 3G), indicating that they were biologically active. Interestingly, although shRNA Pten.932 was more potent than shRNA Pten.5331 in the preinjected cell population, the resulting tumors

Identification and Validation of Previously Uncharacterized Tumor Suppressors

Next, we systematically determined the representation of shRNAs contained within all 31 tumors (derived from seven shRNA pools) that showed accelerated tumor growth (Figure 3B; Table S2). From a total of 2307 sequence reads, we identified 36 shRNAs that were enriched at least 2.5-fold over the predicted representation in the initial plasmid pool (∼2% of total). For example, the two validated *Pten* shRNAs ranked the 5th and 16th, respectively, among the most enriched shRNAs (Table S3). Besides *Pten*, we selected 16 shRNAs targeting
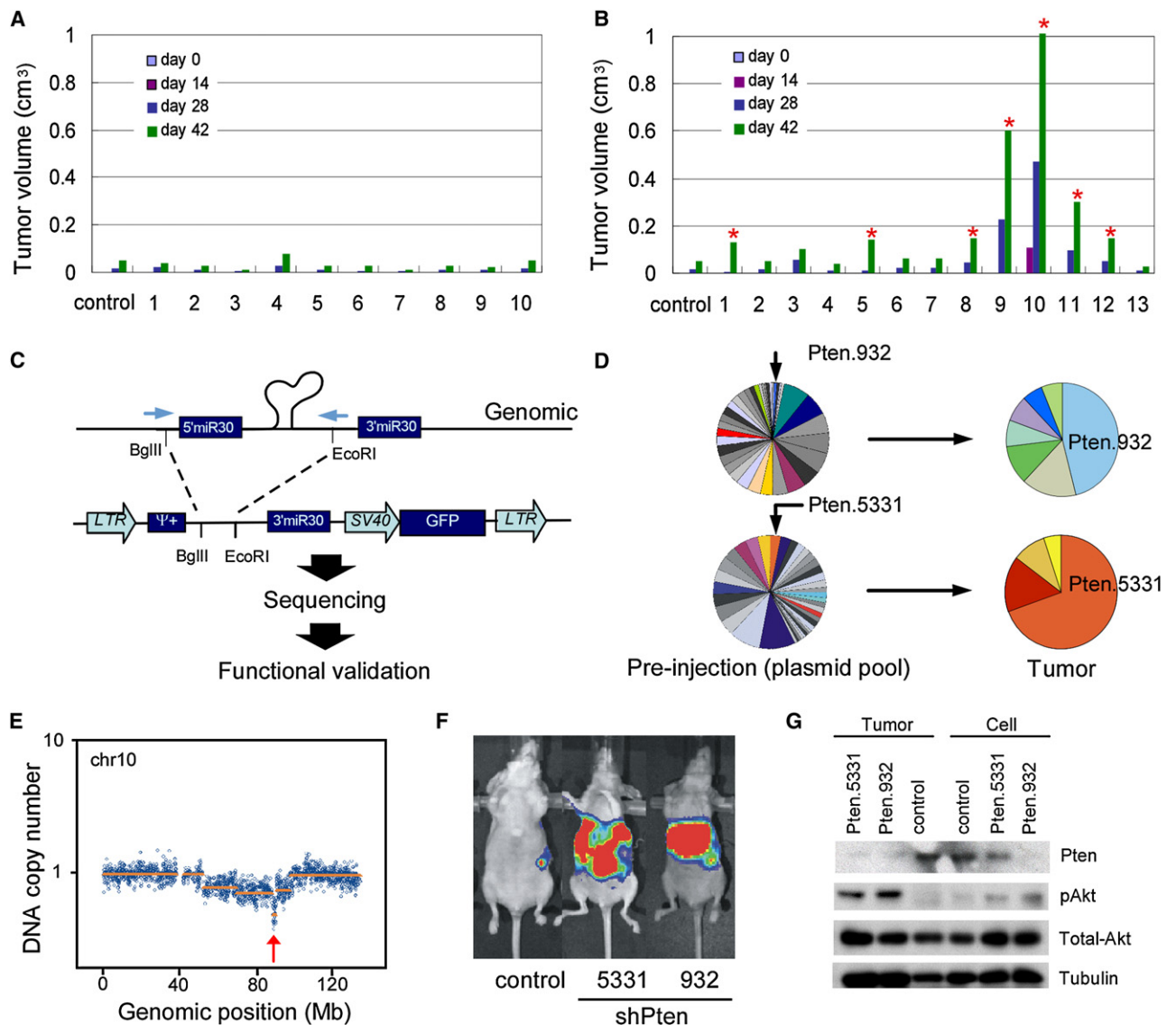
Figure 3. In Vivo shRNA Library Screening Identifies *PTEN* as a Potent Tumor Suppressor in HCC

(A) Average volume (n = 8) of tumors derived from $p53^{-/-};Myc$ cells infected with a control shRNA (control) and ten random genome-wide shRNA pools (pool size n = 48).

(B) Average volume (n = 8) of tumors derived from $p53^{-/-};Myc$ cells infected with a control shRNA (control) and 13 ROMA deletion shRNA pools (pool size n = 48). Red asterisks indicate tumors and shRNA pools subjected to subcloning and sequencing as shown in (C).

(C) Representation of the strategy to recover shRNAs from tumor genomic DNA by PCR and subcloning of the PCR products into the vector used for hairpin validation.

(D) Enrichment of two *Pten* shRNAs in selected tumors (right) compared to their representation in preinjection plasmid pools (left). Pie graphs show the representation of each *Pten* shRNA in the total shRNA population analyzed by high-throughput sequencing.

(E) ROMA arrayCGH plot showing a focal *PTEN* genomic deletion in a human HCC.

(F) Validation of the same *Pten* shRNAs using orthotopically transplanted $P53^{-/-};Myc$ cells transduced with the *Pten* shRNAs. Representative imaging results from three mice in each group are shown.

(G) shRNA-mediated knockdown of Pten increases phospho-Akt. Protein lysates from $p53^{-/-};Myc$ liver cells infected with *Pten* shRNAs (Cell) or the derived tumors (Tumor) were immunoblotted with the indicated antibodies. Tubulin served as a loading control.

14 different genes for validation (Figures 4A and 4B, Table S3). These included all shRNAs that were the most abundant in at least two tumors (targeting *Xpo4*, *Armcx2*, *Nrsn2*, *Zbbx*), all shRNAs for which a second shRNA against the same gene was recovered (targeting *Fgf6*, *Set*, *Fstl5*), and a group of seven addi- tional shRNAs that were also highly enriched (targeting *Wdr49*, *Wdr37*, *Armcx1*, *Gjd4*, *Glo1*, *Ddx20*, *Btbd9*). Interestingly, al- though one candidate target gene, *SET* (histone chaperone and/or protein phosphatase inhibitor), is associated with a rare translocation in acute myeloid leukemia (von Lindern et al.,
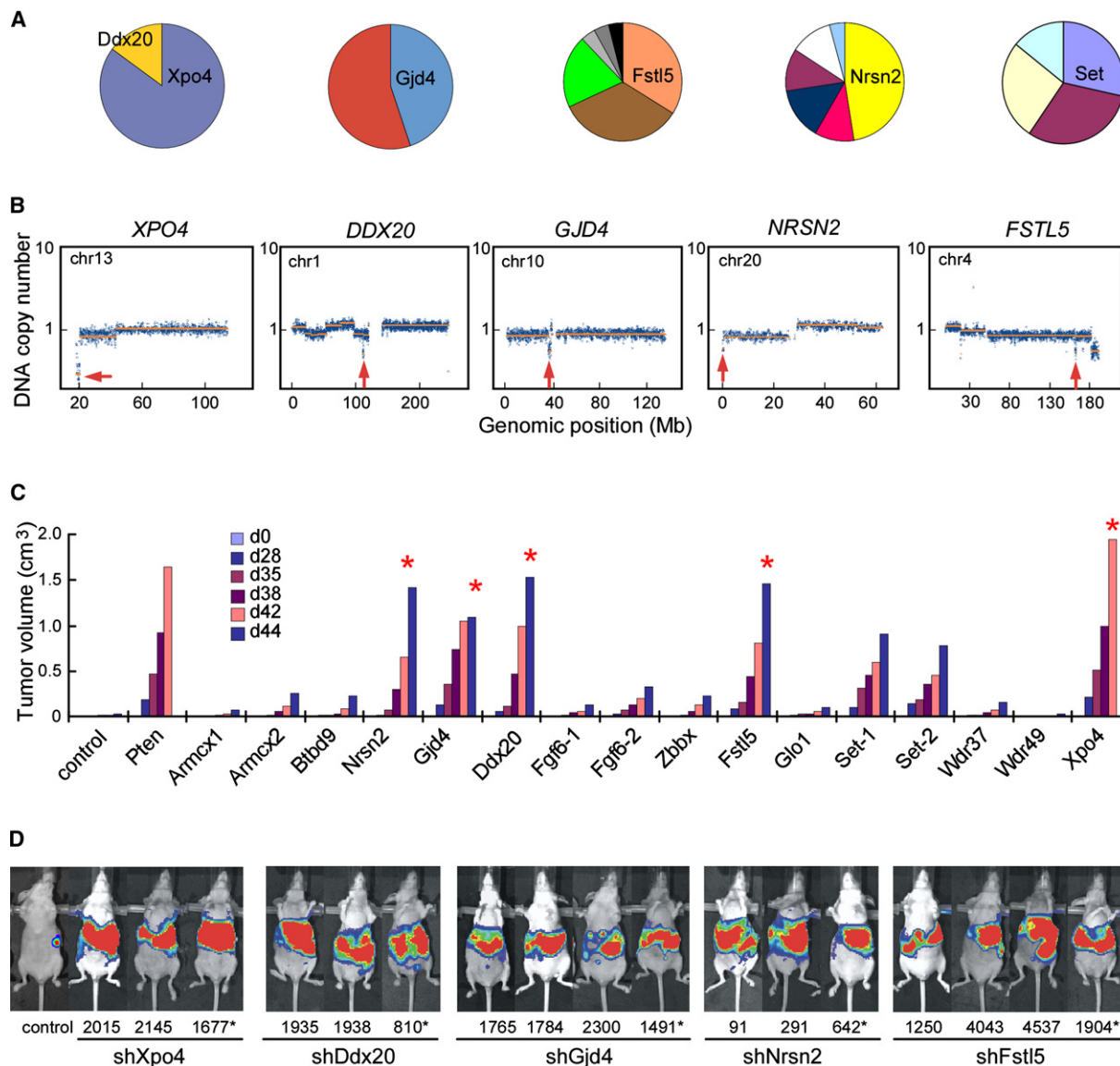
Figure 4. Tumor Suppressor Genes Identified by In Vivo RNAi Screening

(A) Representation of some scoring shRNAs in the tumors. The representation of each shRNA is ~2% in the preinjection plasmid pools, as shown in Figure 3D.

(B) ROMA array CGH plots depicting focal genomic deletions of the genes in (A).

(C) Validation of the top-scoring shRNAs in a subcutaneous tumor growth assay as described in Figure 3F (n = 4). Red asterisks depict genes that were further analyzed in (D).

(D) In situ validation of at least three independent shRNAs targeting genes as depicted in (C). Black asterisks indicate CODEX shRNAs that were initially identified in the screen. Representative bioluminescence imaging results from three mice are shown.

1992), none of the other genes previously have been linked to cancer. Nevertheless, their deletion in a subset of human tumors suggests each could be a relevant tumor suppressor (Figure 4B).

All 16 shRNAs were individually retested with the same experimental setup employed in the initial screen. A validated *Pten* shRNA (Pten.5331) was used as a positive control. Many of the candidate shRNAs triggered tumor growth above background, with those targeting *Xpo4* (nuclear export protein), *Ddx20* (GEMIN3, RNA helicase), *Gjd4* (CX40.1, putative gap junction

protein), *Fstl5* (Follistatin-like 5), and *Nrsn2* (Neurensin 2) showing the most prominent acceleration of tumor growth (Figure 4C). Since our control shRNA never accelerated tumorigenesis, insertional mutagenesis was not solely responsible for the biological effects of our candidate shRNAs—presumably, suppression of the targeted gene was required.

To rule out the possibility that individual shRNAs might promote tumorigenesis through off-target effects, we generated additional shRNAs against each candidate gene and tested them for their ability to promote hepatocarcinoma development
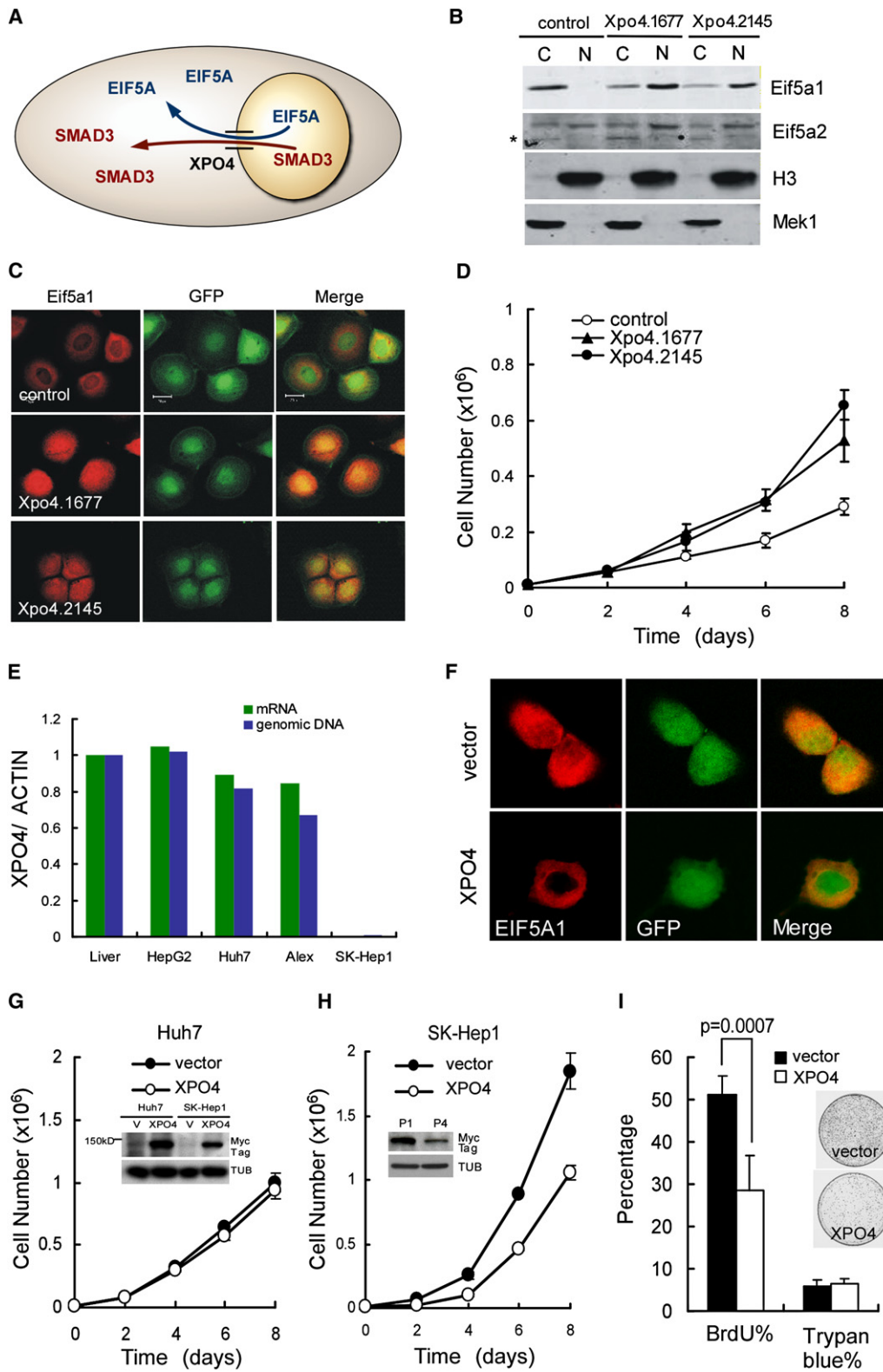
Figure 5. Reintroduction of XPO4 Selectively Suppresses Tumors with XPO4 Deletion
(A) Schematic representation of XPO4 mediated nuclear export of SMAD3 and EIF5A.

in situ. $p53^{-/-}$;Myc liver progenitor cells were transduced with each shRNA, and knockdown of the predicted target gene was confirmed by immunoblotting or quantitative RT-Q-PCR (Figure S4). The resulting cell populations were transplanted into the livers of mice by intrasplenic injection, and recipients were monitored for tumor formation with bioluminescence imaging. At least three independent shRNAs targeting each candidate accelerated tumorigenesis (Figure 4D, see also Figures S5 and S6). Similar results were obtained with independent populations of $p53^{-/-}$;Myc liver progenitor cells (Figure S7). Therefore, genes identified through our in vivo RNAi screen are bona fide tumor suppressors in mice.

Inactivation of XPO4 Deregulates SMAD3 and EIF5A Signaling

The shRNA that was most enriched in our screen targets *Xpo4* (Table S3). Exportin 4 belongs to the importin-β family of nuclear transporters and has two known substrates—SMAD3 and EIF5A (Figure 5A; see also Lipowsky et al. [2000] and Kurisaki et al. [2006]). SMAD3 is an effector of TGF-β signaling that can have pro- or antioncogenic effects depending on context but whose activation is associated with hepatocellular carcinoma progression (Teufel et al., 2007). In response to TGF-β, SMAD3 becomes phosphorylated and shuttles to the nucleus, where it forms complexes with coactivators that transactivate TGF-β target genes (Massagué, 2000). As predicted, murine hepatoma cells expressing *Xpo4* shRNAs showed an increase in nuclear total and phospho-Smad3 (Figure S8A), which correlated with an increase in the levels of the TGF-β target genes *Jun*, *Col7a1*, *Timp1*, and *p15* (Figure S8B).

Although it is straightforward to conceptualize how XPO4 might influence tumorigenesis by modulating SMAD3 function, its biological action on EIF5A is not clear. EIF5A was identified as a eukaryotic translation initiation factor and, in mammals, is encoded by two highly related genes (*EIF5A1* and *EIF5A2*). Although in vitro studies suggest that EIF5A stimulates the formation of the first peptide bond during protein synthesis (Benne and Hershey, 1978), it may also influence nucleocytoplasmatic transport of mRNA and/or mRNA stability (Caraglia et al., 2001). As was observed for Smad3, knockdown of Xpo4 in murine hepatoma cells led to nuclear accumulation of Eif5a1 and Eif5a2 (Figures 5B and 5C), suggesting that Xpo4 may also modulate Eif5a activity.

XPO4 Selectively Suppresses Proliferation in Human Cells with an XPO4 Deletion

Interestingly, Xpo4 shRNAs enhanced the proliferation of murine liver progenitor cells in vitro (Figure 5D). To extend these observations to a human system, we examined how enforced Xpo4 expression affected human HCC cell lines expressing and lacking XPO4 (see Figure 5E for a cell line, SK-Hep1, that does not express XPO4 because of a homozygous deletion). We transduced SK-Hep1 cells (XPO4 negative) and Huh7 cells (XPO4 positive) with a myc-tagged XPO4 cDNA and examined the resulting cell populations for XPO4 expression (Figure 5G, inlay), EIF5A localization (Figure 5F), and proliferation (Figures 5G–5I). The exogenous *XPO4* gene was expressed in both cell types, albeit at higher levels in Huh7 cells (inlays in Figure 5G). Nevertheless, although XPO4 had no impact on the in vitro proliferation of Huh7 cells (Figure 5G), it suppressed SK-Hep1 proliferation (Figure 5H) by delaying cell cycle progression without appreciably promoting apoptosis (Figure 5I). Furthermore, high XPO4 levels produced a selective disadvantage to SK-Hep1 cells since only cells expressing low XPO4 levels could be serially passaged (Figure 5H, inlay). These results extend our findings to a human system, suggest that XPO4 inactivation contributes to tumor maintenance and suggest that XPO4 can limit cell cycle progression.

XPO4 and EIF5A Define an Oncogenic Signaling Circuit

Although the mechanism whereby EIF5A contributes to carcinogenesis is not known, both EIF5A proteins are overexpressed in some human tumors (Clement et al., 2006), and the *EIF5A2* gene is often coamplified with *PIK3CA* (encoding a catalytic subunit of PI3 kinase) on chromosome 3q26 (Guan et al., 2001, 2004). In our data set, we found 22 HCCs with chromosome 3 amplifications that encompass the *EIF5A2* gene (Figure 6A), three of which exclude *PIK3CA*. To determine whether overexpression of EIF5A2, like XPO4 loss, is oncogenic, we retrovirally transduced an *Eif5a2* cDNA into $p53^{-/-}$;Myc hepatocytes and injected the cells subcutaneously into nude mice. Remarkably, Eif5a2, but not Eif5a1, efficiently triggered the growth of tumors (Figure 6B) that displayed histopathological features of hepatocellular carcinoma (data not shown).

To examine the requirement for XPO4 substrates in the proliferation of human tumor cells, we transfected siRNAs targeting EIF5A2 and SMAD3 into HCC cells harboring an *XPO4* deletion (SK-Hep1), *EIF5A2* amplification (Alex), or neither alteration

(B) Eif5a1 and Eif5a2 western blot of cytoplasmic (C) and nuclear (N) fractions of murine HCC cells infected with a control shRNA and two Xpo4 shRNAs. Histone 3 (H3) was used as loading control for the nuclear fraction and Mek1 for the cytoplasmic fraction. * denotes a nonspecific band.

(C) Eif5a1 immunofluorescence in murine HCC cells infected with Xpo4 shRNAs.

(D) Xpo4 shRNAs promote cell proliferation in $p53^{-/-}$;Myc liver cells. Error bars indicate the SD (n = 2).

(E) Expression profile of *XPO4* in human hepatoma cell lines. mRNA abundance and genomic DNA copy numbers of *XPO4* were measured by RT-Q-PCR and genomic Q-PCR. Assays were normalized to actin and to the RNA and DNA from normal liver.

(F) Nuclear accumulation of EIF5A1 in *XPO4*-deficient cells is reverted by reintroduction of *XPO4* cDNA. EIF5A1 immunofluorescence of human HCC cell line SK-Hep1 (XPO4 deleted) infected with control vector or *XPO4* cDNA.

(G and H) Reintroduction of *XPO4* cDNA into *XPO4*-deficient cells inhibits cell proliferation. Cell growth curves of XPO4-postive (Huh7, [G]) and XPO4-negative (SK-Hep1, [H]) human hepatoma cells infected with control vector or *XPO4* cDNA. Error bars indicate the SD (n = 2). The inlay in (G) shows expression level of the 6xMyc-tagged *XPO4* cDNA at early passage in both cell lines. The inlay in (H) shows XPO4 expression in passage 1 (P1) and passage 4 (P4) SK-Hep1 cells after retroviral infection and puromycin selection.

(I) Percentage of BrdU[+] (proliferating) and Trypan blue[+] (apoptotic) cells in SK-Hep1 cells infected with vector control or Xpo4 cDNA. Error bars indicate the SD (n = 5). Inlay shows colony formation assay of SK-Hep1 cells infected with Xpo4 cDNA.
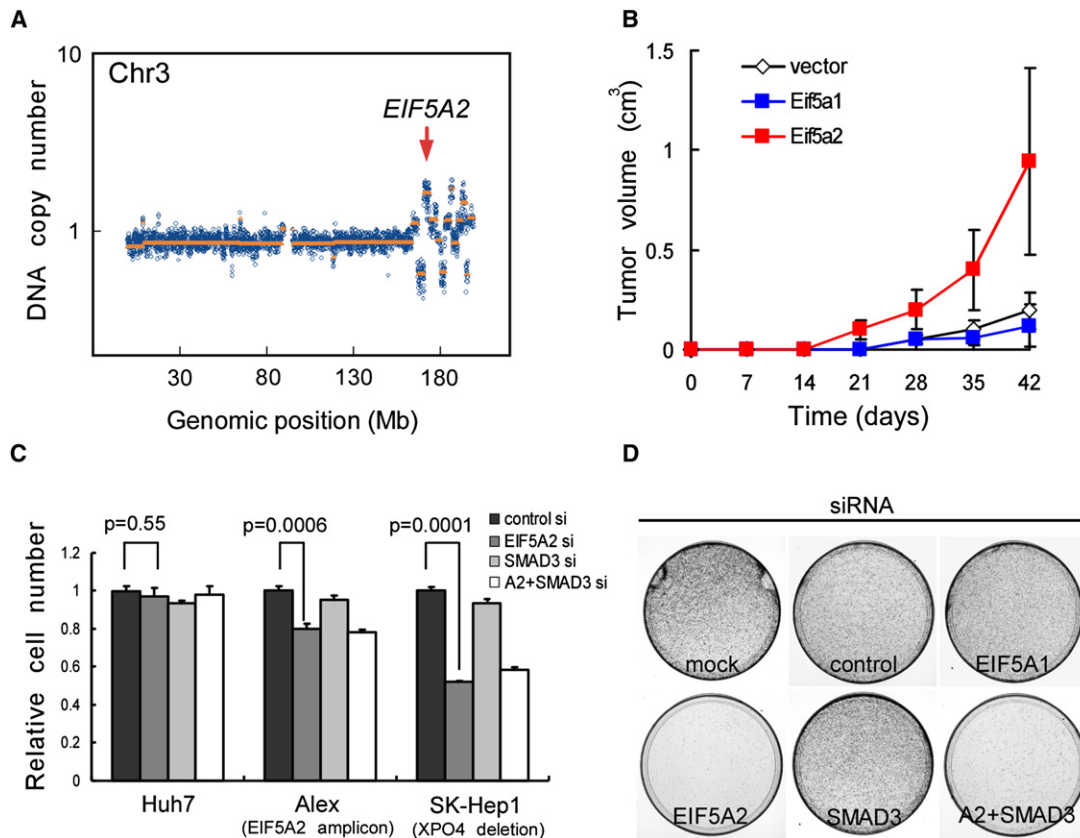
Figure 6. EIF5A2 Is a Key Downstream Effector of XPO4 in Tumor Suppression

(A) ROMA array CGH plot of a human HCC showing an EIF5A2 containing amplicon on chromosome 3.

(B) EIF5A2 expression promotes tumor formation in $p53^{-/-};Myc$ liver progenitor cells. Subcutaneous tumor growth assays were performed as in Figure 2B. Error bars indicate the SD (n = 4).

(C) Knockdown of EIF5A2 attenuates proliferation of human hepatoma cells harboring XPO4 deletion. Cell numbers were measured by MTT assay in human hepatoma cell lines Huh7 (wild-type), Alex (EIF5A2 amplicon) and SK-Hep1 (XPO4 deletion) 48 hr after siRNA transfection. Error bars indicate the SD (n = 3).

(D) Colony formation assay of SK-Hep1 cells transfected with indicated single siRNA or combination.

(Huh7) and examined their impact on short-term (MTT assay) and long-term (colony formation) proliferation. Whereas each set of siRNAs efficiently suppressed their respective target (Figure S9), only siRNAs targeting EIF5A2 inhibited proliferation (Figures 6C and 6D), though these effects were limited to cells that amplified *EIF5A2* or, more prominently, deleted *XPO4* (Figure 6C). Thus, EIF5A2 is required for efficient proliferation in cells lacking XPO4 and may mediate, in part, the oncogenic effects associated with XPO4 loss. Although SMAD3 may also play a role in vivo, these results establish XPO4-EIF5A2 as a regulatory circuit relevant to human cancer.

Genes Identified from Hepatocellular Carcinoma Screens May be Relevant to Other Tumor Types

Hepatocelluar carcinoma shares common biologic and genetic features with other epithelial malignancies. Accordingly, mutations in *APC* and *AXIN* (here used as positive controls) are observed in colon carcinomas, medulloblastomas and other cancers (Segditsas and Tomlinson, 2006; Salahshor and Woodgett, 2005; Teufel et al., 2007), and PTEN (identified in our screen) loss occurs in brain, lung, colon, breast, pancreatic, and prostate cancers (Chow and

Baker, 2006). As a first step in expanding our analyses to other tumor types, we surveyed a database containing copy number analyses of over 257 breast cancers of various pathologies, tumor size, grade, node involvement, and hormone receptor status (Hicks et al., 2006). Gene deletion frequencies were produced from comparative genomic hybridization as described for HCC (Figure 7A); in addition, gene amplification profiles were produced in a parallel manner (Figure 7B). Remarkably, *XPO4* was located at a local deletion epicenter on chromosome 13, which occurs in over 30% of tumors (Figure 7A, see example in Figure 7C) and is associated with poor survival in a large cohort of breast cancer patients (Table S5, p = 0.038). Interestingly, this region often also includes the *Drosophila* tumor suppressor *LATS2* (Yabuta et al., 2000). Of note, shRNAs targeting *LATS2* were not included in our screen as it was not contained in the focal deletions found in liver cancer.

Similarly, the XPO4 substrate *EIF5A2* was near the epicenter of amplifications located on human chromosome 3q26 (Figure 7B, see example in Figure 7D), which is frequently observed in breast cancer. These amplifications were often focal (see Figure 7D) but contained many additional genes. Although the *PIK3CA* gene is a candidate oncogene in this region, at least three breast cancers
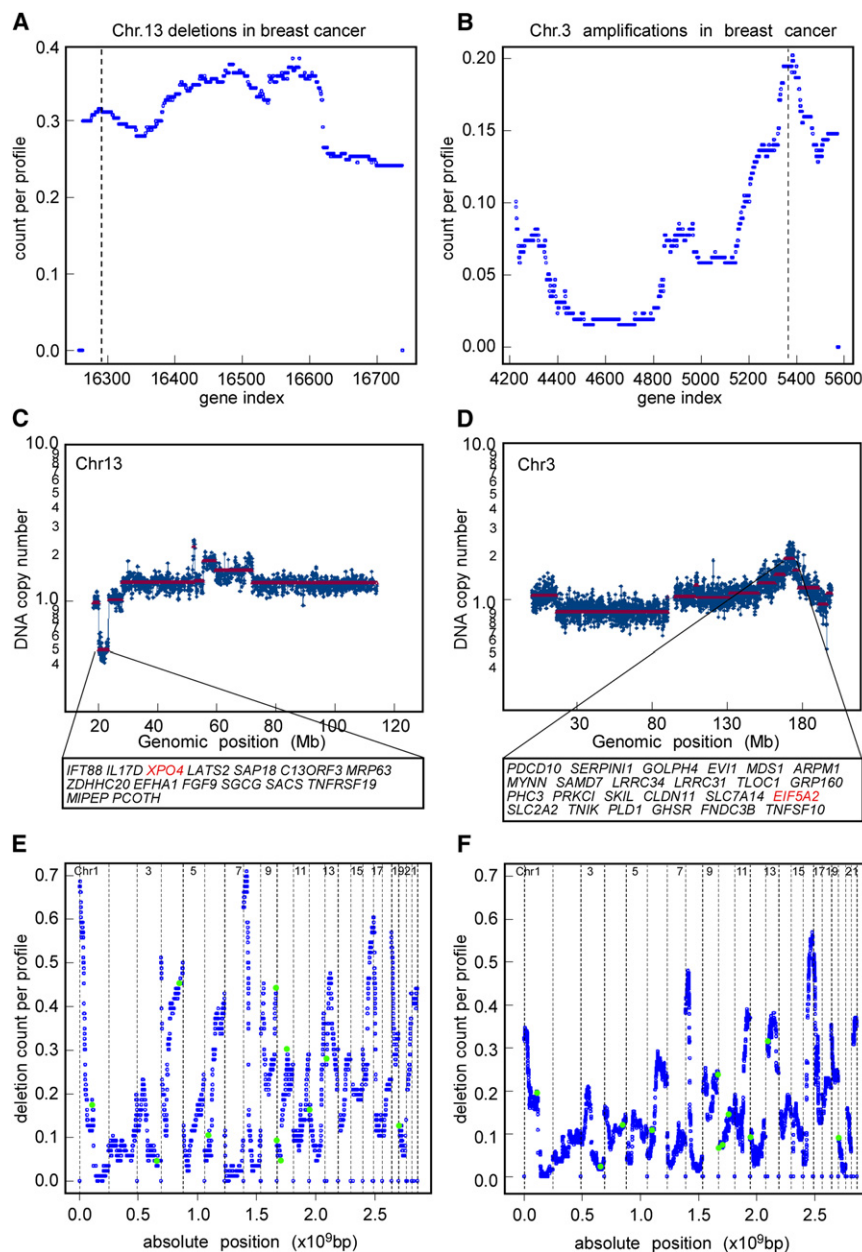
Figure 7. Frequent Copy Number Alterations of *XPO4* and *EIF5A2* in Human Breast Cancer

(A) *XPO4* is frequently deleted in human breast cancer. Shown are the deletion counts in ROMA profiles of 257 human breast cancers with the genes sorted by their genomic transcription start position. Blue dots represent the deletion frequency counts for each gene on chromosome 13. The dashed line points to *XPO4*.

(B) *EIF5A2* is frequently amplified in human breast cancer. Amplification counts (as described in [A]) of chromosome 3 in human breast cancer. The dashed line points to *EIF5A2*.

(C) ROMA plot of a 3.3 Mb *XPO4* deletion in a human breast cancer cell line.

(D) ROMA plot of a 5.8 Mb spanning *EIF5A2* amplicon in a human breast carcinoma.

(E) Genomic distribution of scoring genes from the in vivo RNAi screen. Blue dots denote the deletion frequency count (98 human HCC) for each gene in the genome. Green dots depict the 13 scoring genes (embedded in 11 focal deletions) from the HCC RNAi screen. Dashed lines represent chromosome boundaries. Note: *ARMCX1/2* on the X chromosome are not included.

(F) Tumor suppressor genes identified through the HCC in vivo RNAi screen are also frequently deleted in human breast cancer. Green circles depict the newly identified tumor suppressor genes in a deletion count frequency plot of 257 human breast cancers.

containing the 3q26 amplicon did not amplify *PIK3CA.* Together with our functional analysis, these observations suggest that *EIF5A2* may be an important human oncogene (see also Guan et al., 2004). Several other validated tumor suppressors identified in our HCC screen (Figure 7E) were also located in focal deletions in human breast cancer (Figure 7F), including *PTEN*, *FGF6*, *NRSN2*, and *GLO1/BTBD9* (Table S4). Therefore, although our screen focused on hepatocellular carcinoma, the tumor suppressors we identified may be relevant to other tumor types.

DISCUSSION

This study describes an RNAi screen for genes that affect a complex phenotype in mice. Specifically, to identify new tumor suppressor genes, we performed an oncogenomics-directed RNAi screen for shRNAs that promote tumorigenesis in a mouse model of hepatocellular carcinoma. Our approach was based on the premise that chromosomal regions lost in human cancers are enriched for tumor suppressor genes, and, indeed, we show that pools of shRNAs corresponding to genes deleted in human hepatocellular carcinoma frequently "score" in tumor promotion, whereas pools containing random shRNAs do not. By identifying and retesting those shRNAs that were enriched in the resulting tumors, we validated 13 genes whose suppression reproducibly promotes tumorigenesis in mice. Given that some tumor suppressors were likely missed owing to the absence of an effective shRNA in our library, this approach was remarkably efficient.

The fact that our deletion-specific RNAi pools were enriched for tumorigenic shRNAs implies that many of the genomic deletions observed in human tumors produce a selective advantage and are not "passenger" lesions coincidentally linked to oncogenesis. This notion also explains why some cancer-associated deletions occur repeatedly in different tumor types. Still, we imagine that some loci are particularly susceptible to deletion, for example, at fragile sites, and can be subject to recurrent deletions that do not confer any selective advantage (Durkin et al.,

2008). Although such instability provides one explanation for why we did not identify a driving event for each deletion examined in our screen, our studies document the value of using genomic deletions as filters for identifying new tumor suppressor genes.

Surprisingly, three of the ten focal deletions that scored in our system contain multiple genes whose knockdown accelerates tumorigenesis in mice. Moreover, *XPO4* and *EIF5A2* are adjacent to a strong candidate tumor suppressor (*LATS2*) and oncogene (*PIK3CA*), respectively. That some genomic regions can contain closely linked cancer genes is not unprecedented; for example, the 11q22 amplicon found in human liver cancer and other tumor types contains two genes—*BIRC2* and *YAP*—whose overexpression can cooperate in tumorigenesis (Zender et al., 2006), the *MYC* amplicon on chromosome 8 often coamplifies a noncoding RNA that contributes to cell survival (Guan et al., 2007), and the 14q13 amplicon in lung cancer contains multiple transcription factor oncogenes that cooperate in vitro (Kendall et al., 2007). Conversely, focal deletions on chromosomal region 9p21 often simultaneously codelete the *INK4a* (*CDKN2A*, isoforms 1 and 3), *INK4b* (*CDK2NB*), and *ARF* (*CDKN2A*, isoform 4) tumor suppressor genes, which can act in combination to suppress tumorigenesis (Krimpenfort et al., 2007). The biological rationale for such genomic organization is not understood, but it is possible that these genes are coregulated at the level of higher-order chromatin organization for some purpose during normal cell proliferation or development. Interestingly, shRNAs targeting the linked tumor suppressors identified here were not as potent as others identified in the screen. Although this may be coincidental, future studies will evaluate the combined effects of suppressing these genes on tumorigenesis in mice.

The tumor suppressor genes characterized here target a remarkable array of biological activities. Genes such as *AXIN* (which targets the β-catenin pathway and served as a positive control) as well as *PTEN* (a PI3-kinase pathway regulator identified from the screen) have been implicated in liver cancer based on their somatic alteration in human tumors. Our study therefore solidifies the importance of these genes in liver cancer and develops tractable animal models that may be useful for future functional or preclinical studies. In addition, the *SET* gene, which encodes a histone chaperone and potential protein phosphatase inhibitor, was initially identified as part of a translocation in a human AML patient (von Lindern et al., 1992). Although SET clearly has oncogenic activity in the context of the fusion protein (von Lindern et al., 1992), our studies suggest that the native protein is a tumor suppressor.

By contrast, the vast majority of genes we identified had not previously been linked to cancer. For example, we identified an FGF (*FGF6*), an RNA helicase (*DDX20/ GEMIN3*), a metabolic enzyme (*GLO1*), and *GJD4* (*CX40.1*), a gap junction protein that apparently all act as tumor suppressors in vivo. Some of the genes, for example *FSTL5*, *NRSN2* (*C20ORF98*), and *ZBBX* (*FLJ23049*), are as yet uncharacterized; however, we believe they are relevant to human cancer on the basis of prior evidence for their somatic alteration in human tumors and their impact on tumorigenesis in mice. Clearly, more work will be required to understand how each of these genes suppresses tumorigenesis, and, given the unexpected nature of each gene, such studies may uncover new pathways or principles relevant to cancer.

Our studies utilized *p53* loss *and Myc* as cooperating genetic lesions owing to their common occurrence in human hepatocellular carcinoma, so it is likely that some of the tumor suppressors we identify are specific to this genetic configuration and that others would be identified screening in different genetic contexts. Indeed, some tumor-promoting shRNAs we identified enhance proliferation in the presence of oncogenic Ras, whereas others do not (data not shown). In any case, these results greatly expand our understanding of the genetics of human hepatocelluar carcinoma and point to the potential of nonbiased in vivo RNAi screens to identify potentially new and understudied areas of cancer biology.

Our top-scoring candidate tumor suppressor, exportin 4, belongs to the importin-β superfamily of nuclear transporters and mediates the nuclear export of SMAD3, EIF5A1, and EIF5A2. It seems likely that XPO4 loss contributes to tumorigenesis by promoting the nuclear accumulation of key substrates. Such a possibility is not unprecedented, and indeed, deregulated signaling through the WNT and AKT pathways is thought to influence tumorigenesis by enhancing, or reducing, nuclear accumulation of β-catenin and FOXO, respectively. However, other than rare AML-associated fusion proteins targeting the nuclear pore machinery (Kau et al., 2004), most previously identified mutations affect transport associated signaling pathways and not the nuclear transport machinery itself. That *XPO4* deletions are relatively common suggest that this may be an important mechanism of oncogenesis.

The XPO4 substrates SMAD3 and EIF5A show activities or expression patterns consistent with a role in modulating tumorigenesis. For example, SMAD3 is a modulator of the TGF-β-pathway, which can be anti- or pro-oncogenic depending on context. Although we did not directly examine the extent to which SMAD3 mislocalization contributes to the oncogenic effects of XPO4 loss, we observed that suppression of XPO4 stimulates TGF-β signaling, which can promote invasion and metastasis in late-stage liver cancer (Teufel et al., 2007). Similarly, EIF5A2 overexpression occurs in many tumor types (Clement et al., 2003, 2006). EIF5A was initially purified from rabbit reticulocytes as a translation initiation factor but may have other activities (Caraglia et al., 2001). We see that XPO4 loss enhances proliferation through EIF5A2, which is itself oncogenic in mice. Furthermore, XPO4 re-expression in *XPO4*-deficient tumor cells inhibits proliferation, suggesting these cells depend on XPO4 loss. Our results indicate that XPO4 is a negative regulator of EIF5A2 that acts, presumably in the nucleus, to inhibit cellular proliferation. Therefore, although a precise biochemical mechanism remains to be determined, the XPO4-EIF5A2 signaling circuit appears relevant in hepatocellular carcinoma and other tumor types.

Some of the genes we identify point toward new strategies for cancer therapy. For example, several new tumor suppressors (here, FGF6 and FSTL5) encode secreted proteins whose systemic administration might restore tumor suppressor function and serve as new biological anticancer therapies. Moreover, although it may not be possible to directly restore XPO4 function to tumors, its inactivation leads to hyperactivation of SMAD3/ TGF-β signaling and in principle may sensitize cells to SMAD3 inhibitors, now in clinical trials (Lahn et al., 2005). Furthermore, our studies suggest that EIF5A2 inhibition should have antitumor

effects in XPO-4-deficient tumors. Of note, EIF5A1 and EIF5A2 are the only eukaryotic proteins containing the polyamine derived amino acid hypusine [N^ϵ-(4-amino-2-hydroxybutyl)lysine], which is required for their activity (Park et al., 1994) and whose biogenesis can be inhibited by small molecule drugs that have antiproliferative effects in vitro (Park et al., 1994). Since XPO4 loss is associated with poor survival in breast cancer patients (Table S5), agents that target this pathway may be clinically important.

The strategy outlined herein describes an approach to cancer gene discovery. Most current efforts to catalog cancer genes rely solely on genomic approaches. Although powerful, genomic approaches can be expensive and yield candidates based on statistical criteria. Virtually all candidates must be functionally validated in various in vitro or in vivo models, which is slow and likewise expensive. Through incorporation of our screening approach, it is possible to rapidly filter genomic information for genes that impact cancer development in vivo and thus focus follow-up studies on those that might be most clinically useful. Although our study used a mouse model of hepatocellular carcinoma and focused only on focal deletions, this relatively high-throughput approach could be expanded to other mouse models or include shRNA pools targeting genes affected by larger deletions, promoter methylation, or point mutations. Moreover, through exploitation of the emerging libraries of full-length cDNAs, it should be possible to perform parallel screens for oncogenes involved in genomic amplifications. We believe that such integrative approaches will provide a cost-effective strategy for functional annotation of the cancer genome.

EXPERIMENTAL PROCEDURES

Representational Oligonucleotide Microarray Analysis "ROMA"

Eighty-six HCC tumors and 12 HCC cell lines from the Cooperative Human Tissue Network (CHTN), Hannover Medical School, and the University of Hong Kong have been analyzed by ROMA array-CGH method to generate genome-wide DNA copy number profiles at high resolution (Lucito et al., 2003). Focal deletions are defined as segmented DNA copy number $\leq$ 0.75 and size $\leq$ 20 Mb. This analysis detected a total of 130 focally deleted loci, 44 of which were recurrent. The total number of genes within these loci was 3503. In order to reduce the number of genes, we filtered the deletions by size ($\leq$2.6 Mb) and derived a subset of 58 deleted loci containing 362 genes (Table S1). Methods for calculation of gene deletion frequencies are described in the Supplemental Data (see also Xue et al., 2008) (A.K., J.H., and M.W., unpublished data).

shRNA Library Cloning and Vector Construction

miR30 design shRNAs were subcloned from the pSM2 library vector into a murine stem cell virus (MSCV)-SV40-GFP recipient vector in pool sizes of 48. Maintenance of complexity of the resulting pools was verified by sequencing. The coding regions of human *EIF5A1* and *EIF5A2* were PCR cloned from pCMVsport6 (Open Biosystems) into MSCV-IRES-GFP with a 6xMyc-tag. Myc was expressed with MSCV-based retroviral vectors.

Generation of Immortalized Liver Progenitor Cell Populations

Isolation, culture and retroviral infection of murine hepatoblasts were described recently (Zender et al., 2005, 2006). Liver progenitor cells from E18 $p53^{-/-}$ fetal livers were infected with MSCV-based retroviruses expressing Myc-IRES-GFP or Myc-IRES-Luciferase, and established cell populations were derived from two different preparations.

Generation of Liver Carcinomas

Early passage immortalized liver progenitor cells were transduced by retroviruses expressing single shRNAs or shRNA pools. Two million cells were trans-planted into livers of female C57BL/6 or NCR nu/nu mice (6–8 weeks of age) by intrasplenic injection or injected subcutaneously on NCR nu/nu mice. Tumor progression was monitored by abdominal palpation, whole-body GFP imaging, and bioluminescence imaging (IVIS system, Xenogen). Subcutaneous tumor volume was measured by caliper and calculated as 0.52 × length × width^2. Bioluminescence imaging was as described (Xue et al., 2007).

Histopathology and Immunohistochemistry

Histopathological evaluation of murine liver carcinomas was performed by an experienced pathologist (P.S.) with paraffin-embedded liver tumor sections stained with hematoxylin and eosin (H&E). β-catenin antibody (BD Biosciences, 1:100) staining was performed via standard protocols on paraffin-embedded liver tumor sections.

Immunoblotting and Nuclear Fractionation

Fresh tumor tissue or cell pellets were lysed in Laemmli buffer with a tissue homogenizer. Equal amounts of protein (16 μg) were separated on 10% SDS-polyacrylamide gels and transferred to polyvinylidene fluoride membranes. Nuclear fractionation was performed as described (Hosking et al., 2007). Antibodies are listed in the Supplemental Data.

Immunofluorescence Microscopy

Cells were fixed in 4% paraformaldehyde in PBS for 20 min and permeabilized with 0.2% Triton X-100 in PBS for 5 min. Fixed cells were blocked with 5% goat serum and incubated with primary antibodies for 1 hr and then with goat-anti-mouse Alexa 568 or goat-anti-rabbit Alexa 488 secondary antibodies for 1 hr with washing in between. Microscopy was done with a confocal microscope (Zeiss).

Tissue Culture, RNA Analysis, and Retroviral Gene Transfer

Retroviral-mediated gene transfer was performed with Phoenix packaging cells (G. Nolan, Stanford University, Stanford, CA) as described (Schmitt et al., 2002). Population doubling, BrdU staining, and colony formation assays were as described. RNA expression analysis and PCR primers are described in the Supplemental Data.

SUPPLEMENTAL DATA

Supplemental Data include Supplemental Experimental Procedures, nine figures, and five tables and can be found with this article online at http://www.cell.com/supplemental/S0092-8674(08)01302-0.

REFERENCES

Benne, R., and Hershey, J.W. (1978). The mechanism of action of protein synthesis initiation factors from rabbit reticulocytes. J. Biol. Chem. *253*, 3078–3087.

Caraglia, M., Marra, M., Giuberti, G., D'Alessandro, A.M., Budillon, A., Del Prete, S., Lentini, A., Beninati, S., and Abbruzzese, A. (2001). The role of eukaryotic initiation factor 5A in the control of cell proliferation and apoptosis. Amino Acids 20, 91–104.

Chin, L., and Gray, J.W. (2008). Translating insights from the cancer genome into clinical practice. Nature 452, 553–563.

Chow, L.M., and Baker, S.J. (2006). PTEN function in normal and neoplastic growth. Cancer Lett. 241, 184–196.

Clement, P.M., Henderson, C.A., Jenkins, Z.A., Smit-McBride, Z., Wolff, E.C., Hershey, J.W., Park, M.H., and Johansson, H.E. (2003). Identification and characterization of eukaryotic initiation factor 5A-2. Eur. J. Biochem. 270, 4254–4263.

Clement, P.M., Johansson, H.E., Wolff, E.C., and Park, M.H. (2006). Differential expression of eIF5A-1 and eIF5A-2 in human cancer cells. FEBS J. 273, 1102–1114.

Dickins, R.A., Hemann, M.T., Zilfou, J.T., Simpson, D.R., Ibarra, I., Hannon, G.J., and Lowe, S.W. (2005). Probing tumor phenotypes using stable and regulated synthetic microRNA precursors. Nat. Genet. 37, 1289–1295.

Durkin, S.G., Ragland, R.L., Arlt, M.F., Mulle, J.G., Warren, S.T., and Glover, T.W. (2008). Replication stress induces tumor-like microdeletions in FHIT/FRA3B. Proc. Natl. Acad. Sci. USA 105, 246–251.

Greenman, C., Stephens, P., Smith, R., Dalgliesh, G.L., Hunter, C., Bignell, G., Davies, H., Teague, J., Butler, A., Stevens, C., et al. (2007). Patterns of somatic mutation in human cancer genomes. Nature 446, 153–158.

Guan, X.Y., Sham, J.S., Tang, T.C., Fang, Y., Huo, K.K., and Yang, J.M. (2001). Isolation of a novel candidate oncogene within a frequently amplified region at 3q26 in ovarian cancer. Cancer Res. 61, 3806–3809.

Guan, X.Y., Fung, J.M., Ma, N.F., Lau, S.H., Tai, L.S., Xie, D., Zhang, Y., Hu, L., Wu, Q.L., Fang, Y., and Sham, J.S. (2004). Oncogenic role of eIF-5A2 in the development of ovarian cancer. Cancer Res. 64, 4197–4200.

Guan, Y., Kuo, W.L., Stilwell, J.L., Takano, H., Lapuk, A.V., Fridlyand, J., Mao, J.H., Yu, M., Miller, M.A., Santos, J.L., et al. (2007). Amplification of PVT1 contributes to the pathophysiology of ovarian and breast cancer. Clin. Cancer Res. 13, 5745–5755.

Hemann, M.T., Fridman, J.S., Zilfou, J.T., Hernando, E., Paddison, P.J., Cordon-Cardo, C., Hannon, G.J., and Lowe, S.W. (2003). An epi-allelic series of p53 hypomorphs created by stable RNAi produces distinct tumor phenotypes in vivo. Nat. Genet. 33, 396–400.

Hicks, J., Krasnitz, A., Lakshmi, B., Navin, N.E., Riggs, M., Leibu, E., Esposito, D., Alexander, J., Troge, J., Grubor, V., et al. (2006). Novel patterns of genome rearrangement and their association with survival in breast cancer. Genome Res. 16, 1465–1479.

Horie, Y., Suzuki, A., Kataoka, E., Sasaki, T., Hamada, K., Sasaki, J., Mizuno, K., Hasegawa, G., Kishimoto, H., Iizuka, M., et al. (2004). Hepatocyte-specific Pten deficiency results in steatohepatitis and hepatocellular carcinomas. J. Clin. Invest. 113, 1774–1783.

Hosking, C.R., Ulloa, F., Hogan, C., Ferber, E.C., Figueroa, A., Gevaert, K., Birchmeier, W., Briscoe, J., and Fujita, Y. (2007). The transcriptional repressor Glis2 is a novel binding partner for p120 catenin. Mol. Biol. Cell 18, 1918–1927.

Kau, T.R., Way, J.C., and Silver, P.A. (2004). Nuclear transport and cancer: From mechanism to intervention. Nat. Rev. Cancer 4, 106–117.

Kendall, J., Liu, Q., Bakleh, A., Krasnitz, A., Nguyen, K.C., Lakshmi, B., Gerald, W.L., Powers, S., and Mu, D. (2007). Oncogenic cooperation and coamplification of developmental transcription factor genes in lung cancer. Proc. Natl. Acad. Sci. USA 104, 16663–16668.

Krimpenfort, P., Ijpenberg, A., Song, J.Y., van der Valk, M., Nawijn, M., Zevenhoven, J., and Berns, A. (2007). p15Ink4b is a critical tumour suppressor in the absence of p16Ink4a. Nature 448, 943–946.

Kurisaki, A., Kurisaki, K., Kowanetz, M., Sugino, H., Yoneda, Y., Heldin, C.H., and Moustakas, A. (2006). The mechanism of nuclear export of Smad3 involves exportin 4 and Ran. Mol. Cell. Biol. 26, 1318–1332.

Lahn, M., Kloeker, S., and Berry, B.S. (2005). TGF-beta inhibitors for the treatment of cancer. Expert Opin. Investig. Drugs 14, 629–643.

Lee, J.S., and Thorgeirsson, S.S. (2006). Comparative and integrative functional genomics of HCC. Oncogene 25, 3801–3809.

Lipowsky, G., Bischoff, F.R., Schwarzmaier, P., Kraft, R., Kostka, S., Hartmann, E., Kutay, U., and Görlich, D. (2000). Exportin 4: A mediator of a novel nuclear export pathway in higher eukaryotes. EMBO J. 19, 4362–4371.

Lucito, R., Healy, J., Alexander, J., Reiner, A., Esposito, D., Chi, M., Rodgers, L., Brady, A., Sebat, J., Troge, J., et al. (2003). Representational oligonucleotide microarray analysis: A high-resolution method to detect genome copy number variation. Genome Res. 13, 2291–2305.

Massagué, J. (2000). How cells read TGF-beta signals. Nat. Rev. Mol. Cell Biol. 1, 169–178.

Park, M.H., Wolff, E.C., Lee, Y.B., and Folk, J.E. (1994). Antiproliferative effects of inhibitors of deoxyhypusine synthase. Inhibition of growth of Chinese hamster ovary cells by guanyl diamines. J. Biol. Chem. 269, 27827–27832.

Salahshor, S., and Woodgett, J.R. (2005). The links between axin and carcinogenesis. J. Clin. Pathol. 58, 225–236.

Schmitt, C.A., Fridman, J.S., Yang, M., Baranov, E., Hoffman, R.M., and Lowe, S.W. (2002). Dissecting p53 tumor suppressor functions in vivo. Cancer Cell 1, 289–298.

Segditsas, S., and Tomlinson, I. (2006). Colorectal cancer and genetic alterations in the Wnt pathway. Oncogene 25, 7531–7537.

Silva, J.M., Li, M.Z., Chang, K., Ge, W., Golding, M.C., Rickles, R.J., Siolas, D., Hu, G., Paddison, P.J., Schlabach, M.R., et al. (2005). Second-generation shRNA libraries covering the mouse and human genomes. Nat. Genet. 37, 1281–1288.

Teufel, A., Staib, F., Kanzler, S., Weinmann, A., Schulze-Bergkamen, H., and Galle, P.R. (2007). Genetics of hepatocellular carcinoma. World J. Gastroenterol. 13, 2271–2282.

Tokunaga, E., Oki, E., Egashira, A., Sadanaga, N., Morita, M., Kakeji, Y., and Maehara, Y. (2008). Deregulation of the Akt pathway in human cancer. Curr. Cancer Drug Targets 8, 27–36.

Van Dyke, T., and Jacks, T. (2002). Cancer modeling in the modern era: Progress and challenges. Cell 108, 135–144.

Velculescu, V.E. (2008). Defining the blueprint of the cancer genome. Carcinogenesis 29, 1087–1091.

von Lindern, M., Fornerod, M., Soekarman, N., van Baal, S., Jaegle, M., Hagemeijer, A., Bootsma, D., and Grosveld, G. (1992). Translocation t(6;9) in acute non-lymphocytic leukaemia results in the formation of a DEK-CAN fusion gene. Baillieres Clin. Haematol. 5, 857–879.

Wood, L.D., Parsons, D.W., Jones, S., Lin, J., Sjoblom, T., Leary, R.J., Shen, D., Boca, S.M., Barber, T., Ptak, J., et al. (2007). The genomic landscapes of human breast and colorectal cancers. Science 318, 1108–1113.

Xue, W., Zender, L., Miething, C., Dickins, R.A., Hernando, E., Krizhanovsky, V., Cordon-Cardo, C., and Lowe, S.W. (2007). Senescence and tumour clearance is triggered by p53 restoration in murine liver carcinomas. Nature 445, 656–660.

Xue, W., Krasnitz, A., Lucito, R., Sordella, R., Vanaelst, L., Cordon-Cardo, C., Singer, S., Kuehnel, F., Wigler, M., Powers, S., et al. (2008). DLC1 is a chromosome 8p tumor suppressor whose loss promotes hepatocellular carcinoma. Genes Dev. 22, 1439–1444.

Yabuta, N., Fujii, T., Copeland, N.G., Gilbert, D.J., Jenkins, N.A., Nishiguchi, H., Endo, Y., Toji, S., Tanaka, H., Nishimune, Y., and Nojima, H. (2000). Structure, expression, and chromosome mapping of LATS2, a mammalian homologue of the Drosophila tumor suppressor gene lats/warts. Genomics 63, 263–270.

Zender, L., Xue, W., Cordon-Cardo, C., Hannon, G.J., Lucito, R., Powers, S., Flemming, P., Spector, M.S., and Lowe, S.W. (2005). Generation and analysis of genetically defined liver carcinomas derived from bipotential liver progenitors. Cold Spring Harb. Symp. Quant. Biol. 70, 251–261.

Zender, L., Spector, M.S., Xue, W., Flemming, P., Cordon-Cardo, C., Silke, J., Fan, S.T., Luk, J.M., Wigler, M., Hannon, G.J., et al. (2006). Identification and validation of oncogenes in liver cancer using an integrative oncogenomic approach. Cell 125, 1253–1267.